



**HAL**  
open science

## Experimental study of spruce wood reaction to fire in single burning item test

Lucas Terrei, Davood Zeinali, Zoubir Acem, Véronique Marchetti, Paul Lardet, Pascal Boulet, Gilles Parent

► **To cite this version:**

Lucas Terrei, Davood Zeinali, Zoubir Acem, Véronique Marchetti, Paul Lardet, et al.. Experimental study of spruce wood reaction to fire in single burning item test. *Journal of Fire Sciences*, 2022, 40 (4), pp.293-310. 10.1177/07349041221089829 . hal-04454807

**HAL Id: hal-04454807**

**<https://hal.science/hal-04454807>**

Submitted on 13 Feb 2024

**HAL** is a multi-disciplinary open access archive for the deposit and dissemination of scientific research documents, whether they are published or not. The documents may come from teaching and research institutions in France or abroad, or from public or private research centers.

L'archive ouverte pluridisciplinaire **HAL**, est destinée au dépôt et à la diffusion de documents scientifiques de niveau recherche, publiés ou non, émanant des établissements d'enseignement et de recherche français ou étrangers, des laboratoires publics ou privés.

## EXPERIMENTAL STUDY OF SPRUCE WOOD REACTION TO FIRE IN SINGLE BURNING ITEM TEST

Journal:	<i>Journal of Fire Sciences</i>
Manuscript ID	JFS-21-0112.R1
Manuscript Type:	Original Research Article
Date Submitted by the Author:	n/a
Complete List of Authors:	T, Lucas; LEMTA, Zeinali, Davood; LEMTA Acem, Zoubir; LEMTA Marchetti, Véronique; CSTB Lardet, Paul; CSTB Boulet, Pascal; Université de Lorraine, LEMTA Parent, Gilles; LEMTA
Keywords:	Single Burning Item, Cone calorimeter, Wood degradation
Abstract:	The aim of this work is to study and characterize the fire behavior of vertically-oriented spruce wood panels using experiments conducted at the scales of cone calorimeter and Single Burning Item (SBI) tests. Wood panels were exposed to different burner powers for three exposure times. Very thin thermocouples were embedded inside the wood panel to measure the in-depth temperatures while the lateral position of the char front on the exposed surface and the depth of the char layer were also measured for each test. The latter measurement permitted to establish a char depth map according to the burner power and exposure time. It was observed that for a fixed exposure time, the degraded area on the surface grows linearly with the burner power. Finally, a comparison is made between the char front depths measured with the SBI and those measured with the cone calorimeter for similar heat fluxes.

SCHOLARONE™  
Manuscripts

# EXPERIMENTAL STUDY OF SPRUCE WOOD REACTION TO FIRE IN SINGLE BURNING ITEM TEST

Lucas TERREI<sup>a,\*</sup>, Davood ZEINALI<sup>a</sup>, Zoubir ACEM<sup>a</sup>, Véronique MARCHETTI<sup>b</sup>, Paul LARDET<sup>b</sup>,  
Pascal BOULET<sup>a</sup>, Gilles PARENT<sup>a</sup>

<sup>a</sup>Université de Lorraine, CNRS, LEMTA, F-54000 Nancy, France

<sup>b</sup>Université Paris-Est, Centre Scientifique et Technique du Bâtiment (CSTB), France

---

## Abstract

The aim of this work is to study and characterize the fire behavior of vertically-oriented spruce wood panels using experiments conducted at the scales of cone calorimeter and Single Burning Item (SBI) tests. For this purpose, firstly incombustible panels were exposed to burner powers of 15, 20, 30 and 50 kW in the SBI tests to obtain a mapping of the total heat fluxes received by the panel. Subsequently, wood panels were exposed to the same burner powers for exposure times of 15, 20 and 30 minutes. Very thin thermocouples were embedded inside the wood panel to measure accurately the in-depth temperatures while the lateral position of the char front on the exposed surface and the depth of the char layer were also measured for each test. The latter measurement permitted to establish a char depth map according to the burner power and exposure time. Correspondingly, it was observed that for a fixed exposure time, the degraded area on the surface grows linearly with the burner power. Moreover, the in-depth char front position deduced from the 300 °C isotherm was found to comply very well with that obtained from direct measurements. Finally, a comparison is made between the char front depths measured with the SBI and those measured with the cone calorimeter for similar heat fluxes, showing that the corresponding charring rates from these two tests deviate from one another only at low heat fluxes.

*Keywords:* Single Burning Item, cone calorimeter, wood, degradation

---

## INTRODUCTION

In Europe, building materials are subjected to standardized tests which allow classification according to their reaction to fire.<sup>1</sup> One of the most widely used tests in reaction to fire is the Single Burning Item (SBI).<sup>2</sup> The SBI test is an intermediate-scale test between bench-scale tests such as Fire Propagation Apparatus (FPA) test and full-scale test such as ISO Room Corner test.<sup>3</sup> This test simulates a single burning

---

\*Corresponding author: lucas.terrei@univ-lorraine.fr

1  
2  
3 28 item at the bottom of a room corner (like a burning trashcan) using a propane burner to test construction  
4  
5 29 products and to classify them according to their fire reaction. **The performance is evaluated over a period**  
6  
7 30 **of 20 minutes with visual and non-visual observations.** During the experiment, visual observations are  
8  
9 31 recorded regarding the horizontal spread of the flame front and the fall of flaming droplets or particles.  
10  
11 32 Non-visual measurements such as the Heat Release Rate (HRR) are mainly evaluated with oxygen and  
12  
13 33 carbon dioxide analyzers. **Other measurements such as CO or smoke are also possible with the SBI.**  
14  
15 34 According to the results, the materials are then classified into predefined European classes. For this nor-  
16  
17 35 mative test, the HRR provided by the burner is fixed at  $30 \pm 2$  kW, which is restrictive for studying the  
18  
19 36 fire behavior of samples at this intermediate-scale. Beyond the normative framework of this test, the SBI  
20  
21 37 could be useful to study how wood or other materials behave at the intermediate scale (i.e. between the  
22  
23 38 cone calorimeter<sup>4</sup> and the room corner test<sup>3</sup>), varying the experimental conditions, such as the burner  
24  
25 39 power or the exposure time.

26  
27 40 A recent study performed by Zeinali *et al.*<sup>5</sup> characterizes the SBI gas burner against incombustible cal-  
28  
29 41 cium silicate panels. In that study, data is provided regarding the flame height, total heat fluxes and panel  
30  
31 42 temperatures measured at burner powers of 10, 30, and 55 kW. They observed that the flame height of  
32  
33 43 the burner and the measured heat flux increased with the imposed power. Moreover, they showed that  
34  
35 44 the thermal stress produced by the SBI gas burner over the surface of the panels is non-uniform. Zhang  
36  
37 45 *et al.*<sup>6</sup> conducted similar experiments with incombustible panels and measured the burner heat fluxes  
38  
39 46 on the walls as well as the burner flame heights and the conclusions were similar to those of Zeinali *et*  
40  
41 47 *al.*<sup>5</sup> More specifically, Zhang *et al.*<sup>6</sup> reported mean flame heights of 0.81 m and 1.19 m for the burner  
42  
43 48 powers of 30 kW and 55 kW, respectively, while Zeinali *et al.*<sup>5</sup> reported flame heights of 0.87 m and  
44  
45 49 1.12 m for the same burner powers. Zeinali *et al.*<sup>7</sup> have also studied the fire behavior of Medium Density  
46  
47 50 Fiberboard (MDF) panels with a 30 kW burner power. Flame heights were measured and it was observed  
48  
49 51 that the presence of a combustible panel increases the flame height as well as the HRR compared to tests  
50  
51 52 with calcium silicate panels. The propagation of the char front over the surface of the MDF panels was  
52  
53 53 also measured as a function of the exposure time for 30 kW burner power. Lipinskas and Mačiulaitis<sup>8</sup>  
54  
55 54 performed tests with the SBI to compare the charring rate of different wood samples (hardwood and  
56  
57 55 softwood, treated and untreated). They showed that this speed can vary from 0.5 to 0.8 mm. min<sup>-1</sup> for  
58  
59 56 a burner power of 30 kW. Among the 4 types of wood samples, it was observed that the density of the  
60  
61 57 wood (and not the treatment) has the major influence on the char production.

1  
2  
3 58 Many works have studied how the experimental scale changes the fire behavior of materials.<sup>9, 10, 11, 12, 13, 14</sup>  
4  
5 59 The Research Institute of Sweden (formerly SP) tried to correlate the results of cone calorimeter with  
6  
7 60 those of room corner and SBI test using, in the basis of HRR and smoke production.<sup>9</sup> They developed a  
8  
9 61 specific software (Cone Tools) in order to calculate the HRR and the smoke parameters in SBI and room  
10  
11 62 corner tests from the cone calorimeter results. In other experiments, Hansen and Hovde<sup>10</sup> as well as  
12  
13 63 Delichatsios,<sup>11</sup> used ignition times estimated from the cone calorimeter test to predict the flashover time  
14  
15 64 in the ISO Room Corner test. Hakkarainen and Kokkala<sup>12</sup> evaluated the HRR evolution of a material in  
16  
17 65 the early stages of the experiment in the Room Corner test, thanks to the HRR measured with a cone  
18  
19 66 calorimeter at  $50 \text{ kW} \cdot \text{m}^{-2}$ . Axelsson *et al.*<sup>13</sup> showed that the errors related to the determination of HRR  
20  
21 67 in SBI and Room Corner tests are nearly 10 %, discussing data conventionally obtained from SBI tests  
22  
23 68 such as the Fire Growth Rate (FIGRA), the Total Heat Release (THR) and the Smoke Growth Rate  
24  
25 69 (SMOGRA) on sandwich panels.<sup>14</sup> They concluded that “the correlation between full-scale behaviour in  
26  
27 70 the used set-ups and the new SBI data is still not satisfactory”, showing the need for more research to  
28  
29 71 improve understanding of scale changing. Tsantaridis<sup>15</sup> studied the reaction to fire of wood and building  
30  
31 72 products according to tests at different scale. A single comparison of the FIGRA between the SBI test and  
32  
33 73 the cone calorimeter test (with a constant heat flux of  $50 \text{ kW} \cdot \text{m}^{-2}$ ) was performed. A linear correlation  
34  
35 74 was identified even if this correlation should be confirmed with additional experiments. Despite the sig-  
36  
37 75 nificant use of SBI for the classification of building materials, recent research concerning wood products  
38  
39 76 at this scale remains insufficient. At SBI scale, most of the studies are based on the comparison between  
40  
41 77 different wood samples with a burner power fixed at  $30 \text{ kW}$ .<sup>7, 8</sup>  
42  
43 78 Previous studies showed that the comparisons between cone calorimeter and SBI tests were mainly ad-  
44  
45 79 dressed in the basis of HRR and smoke productions. However, few data are available regarding others  
46  
47 80 properties like in-depth temperatures or surface and in-depth char front mapping. In the present work,  
48  
49 81 the SBI test was used beyond its normative framework in order to study and characterize the fire behavior  
50  
51 82 of vertically-oriented spruce wood panels. The tests were conducted with burner powers of 15, 20, 30  
52  
53 83 and 50 kW, for exposure times of 15, 20 and 30 minutes, while the propagation of the char front on the  
54  
55 84 exposed surface and the depth of char in the panels were measured.

52 85 For the tests carried out at 30 kW, thin wire thermocouples embedded in the wood sample were used to  
53  
54 86 measure accurately the in-depth temperature as described in Terrei *et al.*<sup>16</sup> In this paper, the results ob-  
55  
56 87 tained with this method were compared with in-depth temperatures measured by sheathed thermocouples

1  
2  
3 88 to show the benefit of such an implantation.  
4

5 89 The distribution of the total heat fluxes over the surface of the panels was quantified for all the burner  
6  
7 90 powers on incombustible panels using total fluxmeter. Subsequently, the location with the highest heat  
8  
9 91 flux was determined and chosen to make a comparison against the heat fluxes of tests with spruce wood  
10  
11 92 panels. Finally the char depth measured in the SBI tests was compared to that obtained from cone  
12  
13 93 calorimeter tests.  
14

## 15 94 **EXPERIMENTAL SETUP**

### 17 18 95 *The SBI*

19  
20 96 A total of 22 experiments were conducted with the SBI setup<sup>2</sup> using spruce wood with an exposed  
21  
22 97 surface area of 150 cm by 50 cm. Wood samples were glulam panels made with ten battens of spruce  
23  
24 98 wood glued together with melamine-urea-formaldehyde (MUF) resin. The batten section was 5 × 5 cm,  
25  
26 99 so the panel was 5 cm thick, that can be considered to be thermally thick. The sample average density  
27  
28 100 was approximately 490 kg.m<sup>-3</sup>, with an average moisture content of nearly 10 %. Wood panels were  
29  
30 101 stored in a temperature and humidity controlled room. The SBI consists of a frame on which two vertical  
31  
32 102 panels of the studied material are perpendicularly arranged. A propane sand box burner is placed at 4 cm  
33  
34 103 from the corner. The burner is an isosceles right-angled triangle with 25 cm side. The setup is placed in  
35  
36 104 a dedicated test room (3 m × 3 m × 2.4 m), under a hood with a system to continuously extract a flow  
37  
38 105 rate from 0.50 to 0.65 m<sup>3</sup>.s<sup>-1</sup>.  
39  
40  
41  
42  
43  
44  
45  
46  
47  
48  
49  
50  
51  
52  
53  
54  
55  
56  
57  
58  
59  
60

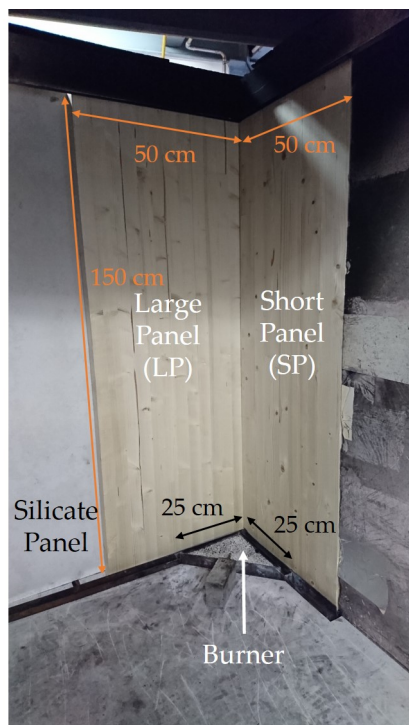


Figure 1: SBI experimental setup.

For the normative test, the two panels exposed to the burner do not have the same dimension. There are one short panel (50 cm × 150 cm) and one large panel (100 cm × 150 cm). This arrangement makes it possible to observe the horizontal spread of the flame during the test. Nevertheless, it was shown by Zeinali *et al.*<sup>7</sup> that the flame spread on the long MDF panel never exceeds 50 cm, i.e. less than the short panel width. So, for this study, two identical panels having a 50 cm width were used. A similar configuration was also chosen by Chaudhari *et al.* on PMMA panels.<sup>17</sup> Additionally, in the present configuration, the remainder of the wall on the large panel side was completed by a 50 cm wide calcium silicate panel to remain in the same configuration to the original SBI test and ensure an air supply similar to the tests carried out in previous works. For the sake of clarity, the labels “large panel” and “short panel” denominations will be still used in the paper as shown in Fig. 1. The spruce panels were exposed to burner HRR values of 15, 20, 30 and 50 kW for exposure times of 15, 20 and 30 minutes. Temperatures inside the wood were measured with K-type thermocouples during the tests. However, depending on how the thermocouples are implanted in the wood sample, the measured temperature can vary by up to 400 °C for some experimental conditions, as shown in.<sup>16,18,19</sup> A precise measurement method was developed recently,<sup>16</sup> consisting in embedding very thin (0.1 mm diameter) wire thermocouples in-

side the sample, along the isotherms parallel to the exposed surface. This method was validated at the small scale with cone calorimeter tests and is implemented here, at the SBI scale. For that, the wood panel was cut perpendicularly to the exposed surface, and then square-grooves with 0.2 mm depth and 0.2 mm width were precisely machined at the desired locations. Then, wire K-type thermocouples composed of alumel and chromel wires were welded by autogenous electric welding and put in the square-grooves. Finally, wood panel was glued with Melamine-Urea-Formaldehyde (MUF). More details concerning the protocol of the thermocouple implantation in the wood sample are presented in.<sup>16</sup> At the scale of SBI, implanting the thermocouple wires in this way takes four hours per sample from grooving to bonding and thermocouple welding. The temperature was only studied for the short panel. Figure 2 shows the position of the thermocouples in the wood sample. The thermocouple junctions (red points in Fig. 2) are placed at 9 cm from the corner line and 45 cm from the bottom of the panel, at a location where the panel should be severely affected by the burner flame.

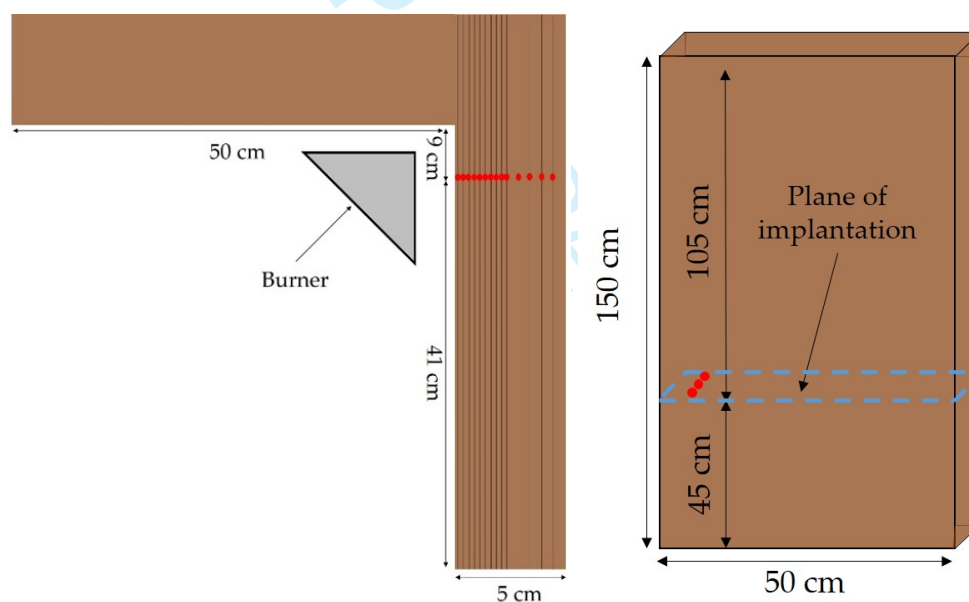


Figure 2: Diagrams showing the in-depth thermocouple measurement points (red circles) inside the wood panel. The top view of the panel is shown to the left, while the side view of the measurement panel is shown to the right.

To verify the importance of how the thermocouples are implanted in the wood sample and assess discrepancies, separate tests were also performed with four K-type sheathed thermocouples (1 mm diameter) placed inside holes drilled on the back side of the sample (i.e., perpendicular to the isotherms) using a 1.5 mm diameter drill bit, respectively at 10, 20, 30 and 40 mm depth from the exposed surface. As



1  
2  
3 137 suggested by Reszka and Torero,<sup>20</sup> the sheathed thermocouples were spaced by 20 mm in order to limit  
4  
5 138 their mutual disturbance.

### 8 139 *The cone calorimeter*

9  
10 140 As introduced by previous studies,<sup>10,11,12</sup> comparisons between the cone calorimeter<sup>4</sup> and the SBI<sup>2</sup>  
11  
12 141 are very useful for the understanding of the fire behavior of materials. The HRR evolution or the time-  
13  
14 142 to-ignition are among the most often used data to identify the correlation between the two scales. In the  
15  
16 143 present work, the char depth positions in the two scales were compared over time. Following the standard  
17  
18 144 ISO 5660-1, the wood samples in the cone calorimeter tests were wrapped with two layers of aluminum  
19  
20 145 foil, and the distance between the heater and the tested samples was 25 mm. For these experiments, the  
21  
22 146 cone heater and wood samples were oriented vertically like for SBI tests, without a pilot flame or spark.  
23  
24 147 The spruce wood material of the cone samples (10 cm × 10 cm × 5 cm) was identical to that tested at  
25  
26 148 intermediate scale. **The incident heat fluxes for the cone calorimeter tests were chosen in order to match**  
27  
28 149 **the SBI heat fluxes measured both with the wood and the incombustible panels.**

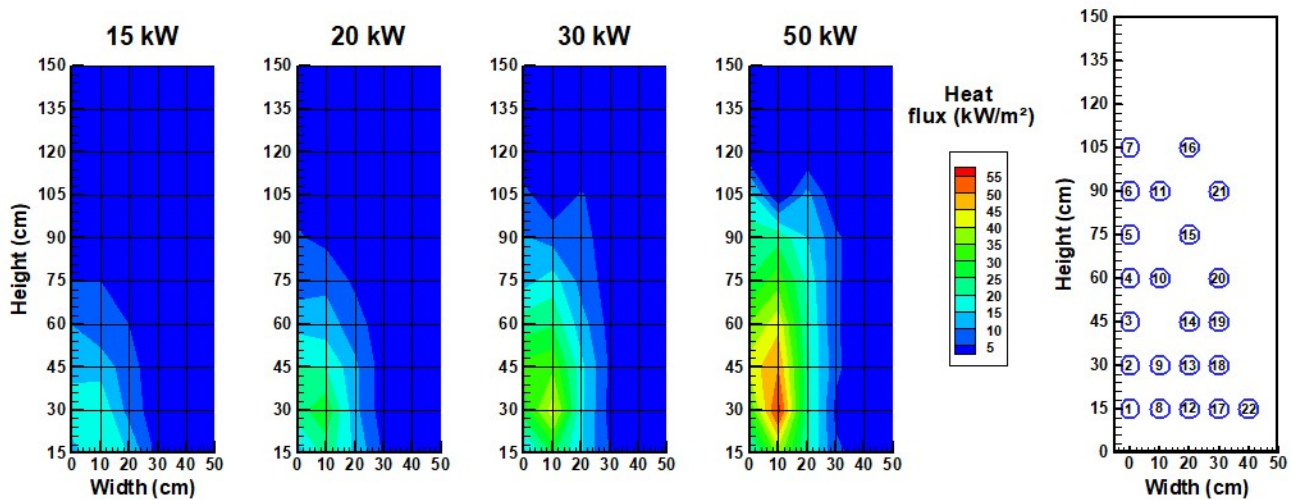
## 29 150 **RESULTS**

30  
31  
32 151 This section firstly presents the results of the SBI tests conducted with incombustible calcium silicate  
33  
34 152 panels (average density:  $870 \pm 50 \text{ kg.m}^{-3}$  and 12 mm thickness), followed by the test results of spruce  
35  
36 153 wood panels in SBI and the cone calorimeter, discussing the heat fluxes, in-depth temperatures, char front  
37  
38 154 on the exposed surface and char front depth in the samples.

### 40 155 *Total incident heat fluxes on incombustible panels in SBI*

41  
42 156 First, an inert calcium silicate panel was exposed to the burner powers equal to 15, 20, 30 and 50 kW,  
43  
44 157 while the total incident heat fluxes were measured with a water-cooled (around 12 °C) heat flux gauge  
45  
46 158 (Gardon type from Captec). This heat flux sensor was placed in holes with a diameter equal to that of  
47  
48 159 the fluxmeter (i.e., 2.5 cm), previously drilled on the short panel at various locations. Figure 3 shows the  
49  
50 160 locations of the gauge and the corresponding mapping of the measured heat fluxes for different burner  
51  
52 161 powers. The free holes were blocked with plugs from the same materials as the panel to prevent any gas  
53  
54 162 flow through them. The heat flux was measured on the small panel at a total of 22 points with locations  
55  
56 163 ranging from 15 to 105 cm along the height and from 0 to 40 cm along the width. For each burner  
57  
58 164 power and measurement point, the heat flux was recorded for 2 minutes. When the burner is ignited, it is

1  
2  
3  
4 165 necessary to wait for approximately 30 seconds before reaching a steady state. As a result, the average  
5  
6 166 of the flux value and its standard deviation were only calculated for the last 90 seconds. The acquisition  
7  
8 167 frequency being 5 Hz, the average was taken over approximately 365 measurements. Figure 3 presents a  
9  
10 map of the heat fluxes obtained for each burner power.



29  
30  
31 Figure 3: Contour plots of total heat fluxes obtained using burner powers of 15, 20, 30 and 50 kW on the incombustible short  
32  
33 panel. The measurements were made using a water-cooled heat fluxmeter at the locations shown on the diagram to the right.

34  
35 169 The heat flux maps illustrated in Fig. 3 show that the heat flux received at the wall increases locally  
36  
37 170 with the power of the burner. For a 50 kW burner power, the measured heat flux is at least  $30 \text{ kW}\cdot\text{m}^{-2}$   
38  
39 171 over a large area (20 cm wide and 85 cm high). **Beyond 105 cm in height and 30 cm in width, the heat**  
40  
41 172 **flux was not measured (except in position 22) but the heat flux does not exceed  $5 \text{ kW}\cdot\text{m}^{-2}$  there.** These  
42  
43 173 measurements are consistent with those obtained in Zhang *et al.*<sup>6</sup> and Zeinali *et al.*<sup>5</sup> works showing the  
44  
45 174 heterogeneity of the irradiance over the sample surface.

#### 175 ***Total incident heat fluxes on the spruce wood panel***

176  
177 The same fluxmeter used in **the previous** section was placed at position 9 shown in Fig. 3, i.e. at a  
178  
179 height of 30 cm and a distance of 10 cm from the corner in order to measure the heat flux on the spruce  
180  
181 wood panel for the burner powers of 15, 20, 30 and 50 kW. It will be possible to observe the additional  
effect of the flame produced by the burning wood by comparing the heat flux received by the two types  
of sample. Figure 4 shows the values of the measured heat fluxes as a function of the imposed burner  
power. The heat fluxes in the wood panel tests were averaged over 15 minutes of testing.

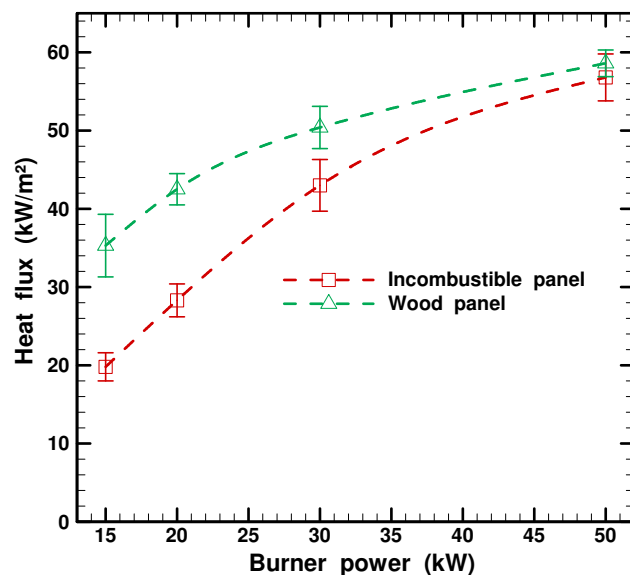


Figure 4: Comparison of the total incident heat fluxes measured on an incombustible panel (squares) and that with a spruce wood panel (triangles) as a function of the burner power.

182 The measurements indicate that the heat flux received by the wooden panel is systematically higher  
 183 than that received by the incombustible panel for the same burner powers (see Fig.4). For a 15 kW burner  
 184 power, the heat flux is increased by 85 % for the wood panel, compared to the inert panel, but only 3 % for  
 185 the 50 kW burner power. This shows that the difference tends to decrease as the heating power increases.  
 186 Indeed, for a low power of the burner, the heat flux received on the panels is mainly radiative since the  
 187 burner flame is too small to stick to the panel surface (more precisely at the fluxmeter's location). For  
 188 a combustible panel, the burning of the panel produces an additional convective heat flux on the panel  
 189 surface, as the pyrolysis gases feed and widen the burner flame. Therefore, the heat fluxes received by  
 190 the combustible panels are significantly larger than those received by the inert panels. This explains the  
 191 large differences in the irradiance of the two types of surface for the 15 and 20 kW tests.  
 192 For higher burner powers, the flame of the burner is large enough to stick to the panel surface so a  
 193 convective flux coming from the burner flame is also present. In this case, the pyrolysis gases feed the  
 194 burner flame but its thickness does increase any further. Moreover, the combustible panels in this case also  
 195 experience the so-called "blowing effect", i.e., reduction of convective heat transfer to the surface due to  
 196 the opposite flow of pyrolyzate mass.<sup>5,21,22</sup> Accordingly, as the burning rate of the panels increases with  
 197 higher burner powers, the convective heat transfer to the surface decrease, just as reported in.<sup>7,23</sup> This

1  
2  
3  
4 198 explains the convergence of the heat fluxes of combustible and incombustible panel tests as the burner  
5  
6 199 power increases **at the position where the heat flux was measured.**

### 8 200 *Surface char front propagation on the wood panels*

9  
10 201 After each test, the wood panels were extinguished with water in order to stop the wood combustion  
11  
12 202 and degradation. The inspection of the samples after the tests shows that the power of the burner plays  
13  
14 203 an important role in the degradation of the wood. Figure 5 presents spruce wood samples after tests at  
15  
16 204 different burner powers for an exposure time of 15 minutes. For the same exposure time, the quantity of  
17  
18 205 char increases with the imposed power.



Figure 5: Photos of test specimens after 15 minutes of testing with burner powers ranging from 15 to 50 kW.

206 As illustrated in Fig. 5, it is possible to define three zones of degradation: (A) the zone next to the  
207 corner line formed by the panels, severely degraded with millimeter-sized cracks (zone A always has char  
208 depths higher than 9 mm); (B) the intermediate zone between the region with large cracks and the region  
209 with no significant cracks (zone B has char depths between 2 and 9 mm); (C) the charred zone farthest  
210 away from the corner line, featuring a minimum level of degradation and no significant cracks (zone C  
211 has char depths between 0 and 1 mm). The width of these three zones were measured for each panel  
212 every 20 cm along the height. Figure 6 presents the boundaries of zones A, B and C on a test specimen  
213 for three tests performed at 20 kW for 30 minutes.

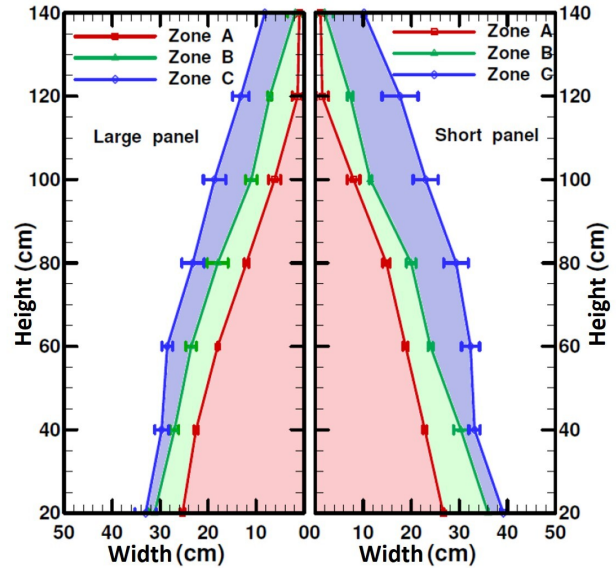
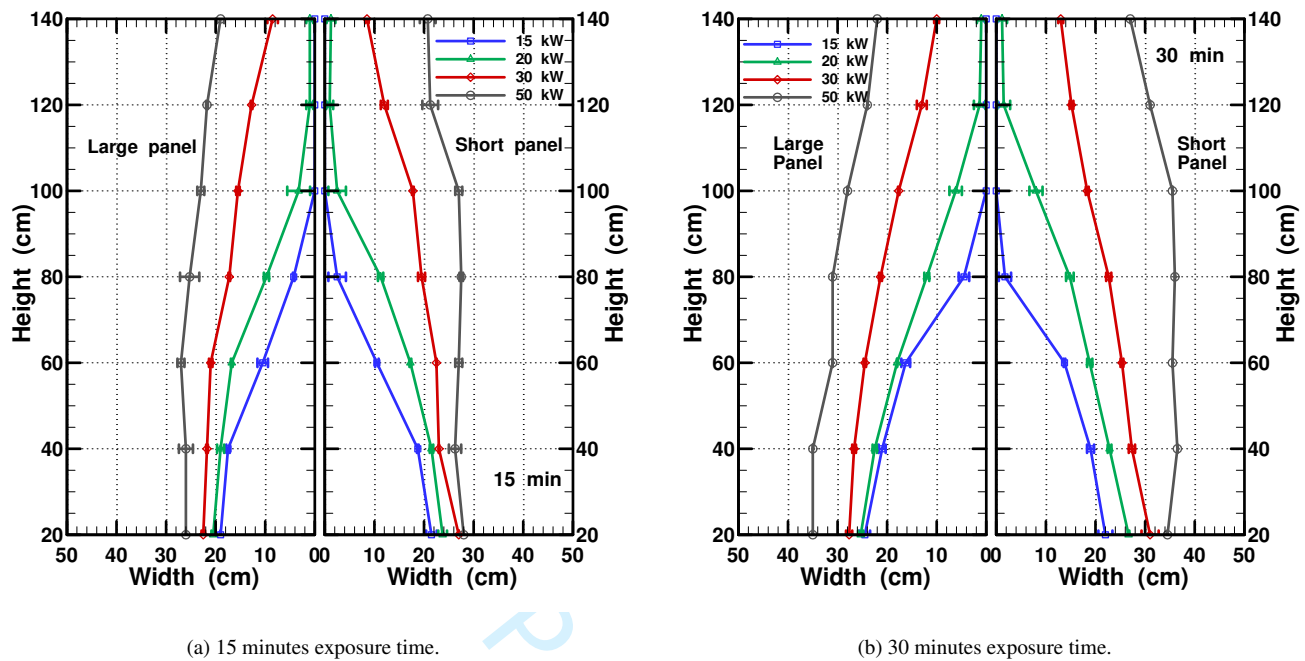


Figure 6: Degradation zones of wood samples for tests conducted with a 20 kW burner power. The error bars indicate the magnitude of one standard deviation across the tests.

Figure 6 also indicates the standard deviation in the positioning of the boundaries of zones A, B and C in the three tests carried out with the spruce wood panels. We can see that the location of zone A is quite repeatable (small error bars) whereas more discrepancies are observed on boundaries of zones B and C. Figure 7 presents the propagation of the char front over the surface in zone A as a function of the burner power for two exposure times, namely 15 and 30 minutes.



(a) 15 minutes exposure time.

(b) 30 minutes exposure time.

Figure 7: Evolution of the surface char front in zone A for different burner powers with exposure times of 15 min (left) and 30 min (right). The error bars indicate the magnitude of one standard deviation across three tests.

For a given exposure time, the propagation of the char front at the surface increases with the burner power. There is also an asymmetry between the degradation patterns of the short panel and those of the large panel. This observation is also confirmed by the char depth, which generally shows that the short panel is more degraded than the large one. This observation concerning the in-depth temperatures and heat fluxes was also observed by Zeinali *et al.*<sup>5</sup> and Zhang *et al.*,<sup>6</sup> and is expected to be due to the air supply pattern in the setup which favors flame spread on the short panel.<sup>23</sup> Indeed, this phenomenon leads to higher temperatures of 100 °C<sup>5</sup> as well as 1 to 5 kW.m<sup>-2</sup> larger heat fluxes<sup>6</sup> on the short side. Figure 8 shows how the area of zone A increases as a function of the imposed burner power.

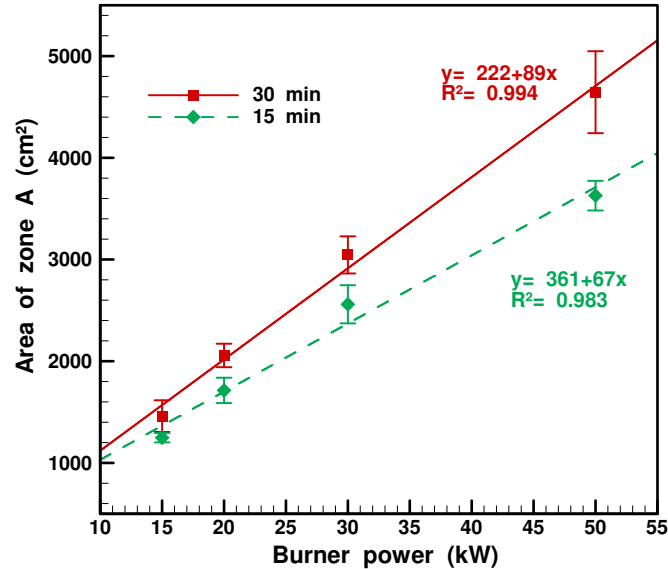


Figure 8: Evolution of the area of zone A as a function of the burner power. The error bars indicate the magnitude of one standard deviation across three experiments.

For a given exposure time, the area of zone A increases almost linearly with the burner power. In other words, the surface of degradation is almost doubled when the burner power is multiplied by two. On the other hand, doubling the exposure time for the burner powers of 15, 30 and 50 kW increases the degradation area of zone A by 15, 20 and 30 %, respectively. This means that the area of zone A does not increase linearly with the exposure time.

### *In-depth panel temperatures*

Figure 9 presents the temperature evolutions for the different depths. The tests were carried out three times for a 30 kW burner power.

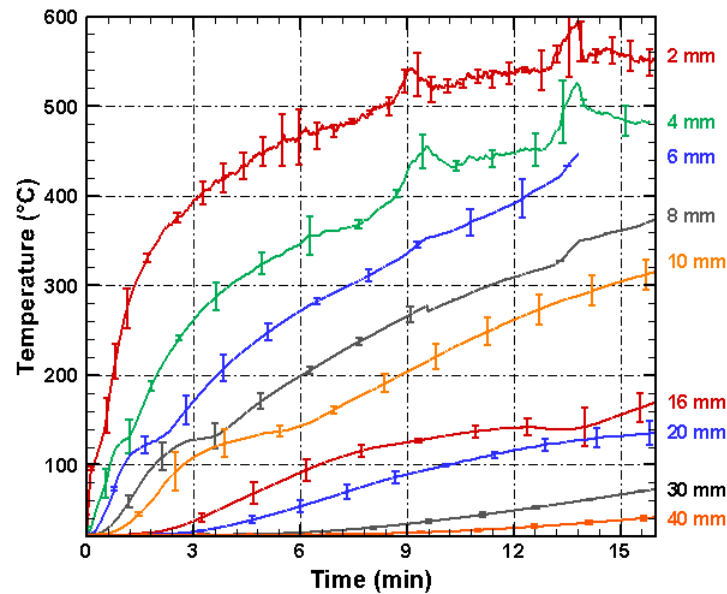


Figure 9: In-depth temperature evolutions measured by embedded wire thermocouples located at 2 to 40 mm depth from the exposed surface for a 30 kW burner power. The error bars indicate the magnitude of one standard deviation across three tests.

On the side exposed to the burner, the in-depth panel temperatures increase rapidly before reaching a slower growing phase. The small error bars, corresponding to the standard deviation values, suggest that the repeatability of the tests is sufficient. At 2 mm depth, the error bars are larger due to the fast heating dynamics. The maximum temperature is 600 °C. Two peaks are present at depths of 2 and 4 mm at exposure times of 9 and 14 minutes, possibly due to the appearance of an incandescent zone close to the measurement sensor. Moreover, there is also an inflection around 120 °C just as observed in cone calorimeter tests.<sup>16</sup> Figure 10 compares the results obtained at the different depths with the sheathed thermocouples (oriented perpendicular to the panel's exposed surface) and the wire thermocouples (oriented parallel to the panel's exposed surface).



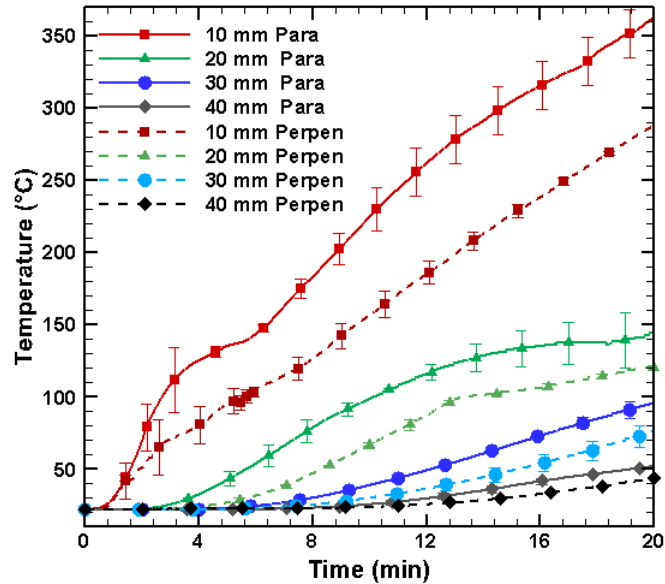


Figure 10: In-depth panel temperatures measured using sheathed thermocouples placed in holes drilled from the back of the panel (dashed lines) and those measured using bare thermocouple wires placed parallel to the isotherms by implantation (solid lines), in tests with a burner power of 30 kW.

As Fig. 10 indicates, the temperature measurements made with sheathed thermocouples placed in holes drilled from the back side show significant differences from the temperatures obtained using bare thermocouple wires implanted along the isotherms. This is the case even for positions that are far from the exposed surface. The temperature at the end of the test at 10 mm depth is 360 °C for the embedded thermocouple against 285 °C for the sheathed thermocouple, i.e., a 75 °C difference. At the depth of 10 mm, it takes more than 6 minutes delay for the two types of thermocouple to record 300 °C (14 minutes for the embedded thermocouple and more than 20 minutes for the sheathed thermocouple). The differences are smaller at 20, 30 and 40 mm depths but still significant.

### *Char front propagation*

Several additional specimens were exposed to 30 kW for 15, 20 and 30 minutes before being cut in half at the thermocouple junctions location (45 cm height and 9 cm from the corner). At this location, the heat flux received is around 35 kW.m<sup>-2</sup> according to Fig. 3, which can be used to make comparisons with cone tests<sup>16</sup> in terms of charring rates. Correspondingly, the char front depth of the panels was measured at this location with a ruler and was compared with the position of the 300 °C isotherm (determined from

258 embedded thermocouples temperature measurements).<sup>16,24</sup> The results are presented in Fig. 11.

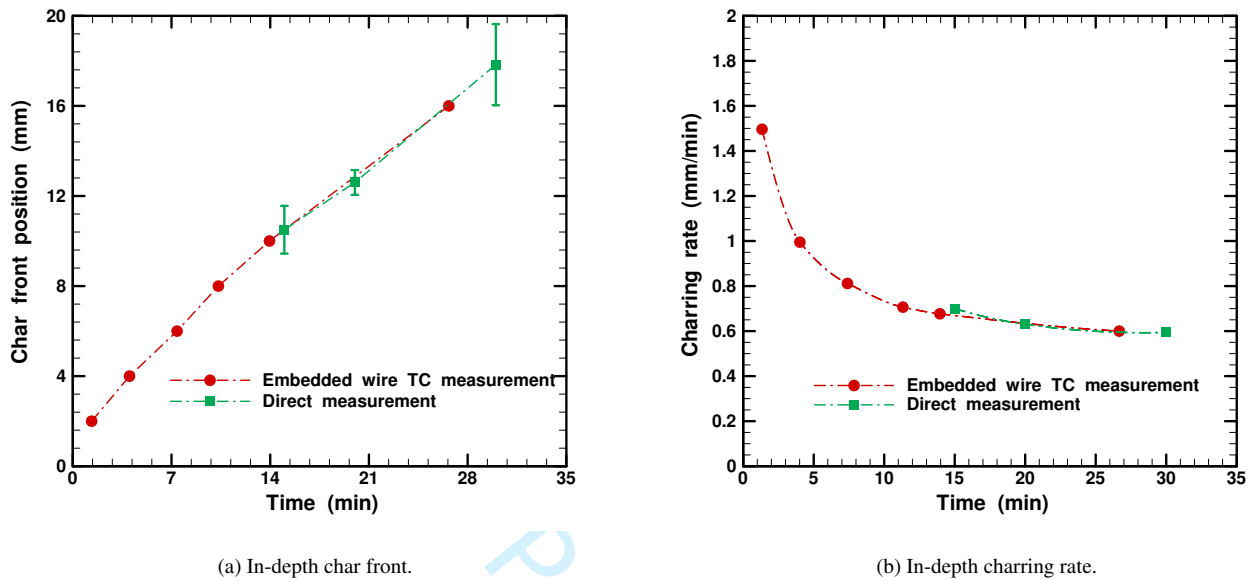
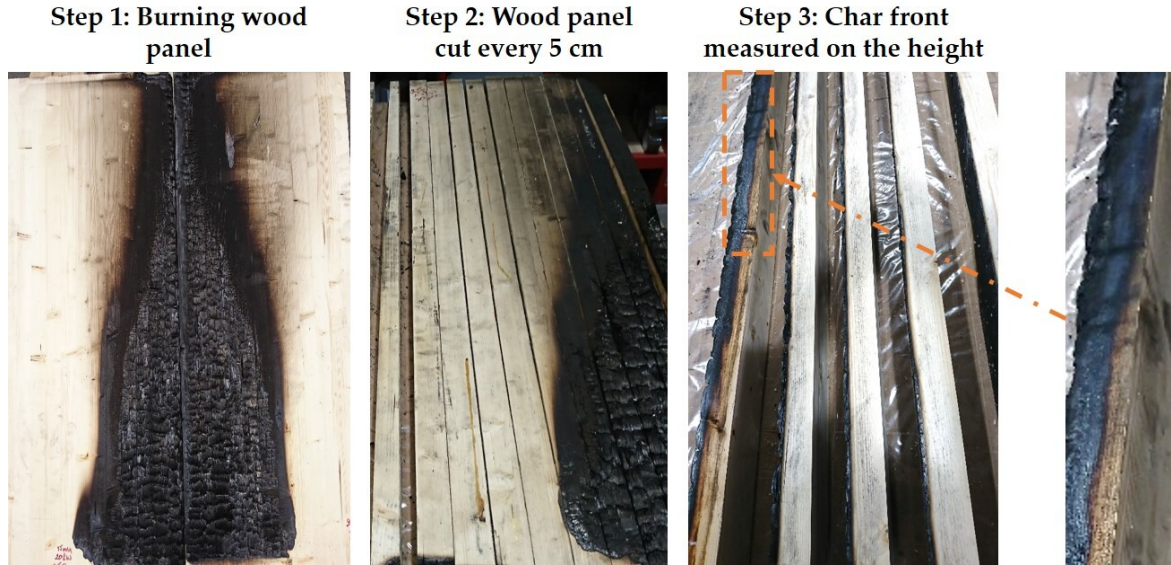


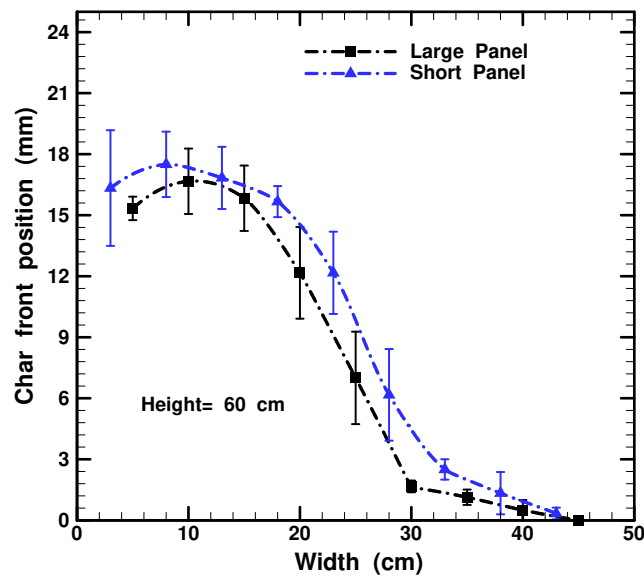
Figure 11: Comparison of the in-depth char front propagation (left) and the deduced charring rate (right), determined either on direct measurements of the char layer thickness (square symbols) or estimated by the 300 °C isotherm measurements made using the embedded thermocouples (circle symbols), with a burner power of 30 kW.

259 The in-depth char front positions determined via direct measurements are in good agreement with  
 260 those estimated by the 300 °C isotherm measurements made using the embedded thermocouples, just  
 261 as observed by Terrei *et al.*<sup>16</sup> The char front reached the depths of 10.5 and 18 mm after the exposure  
 262 times of 15 and 30 min, respectively. It appears that the propagation of the char front slows down with  
 263 time according to a power law, as showed in Fig. 11b. The curve shows that the charring rate is not  
 264 constant during the experiment. It starts at 1.5 mm.min<sup>-1</sup> and decreases rapidly to 0.7 mm.min<sup>-1</sup> after  
 265 10 minutes of exposure. Subsequently, the charring rate becomes more or less constant, staying between  
 266 0.6 and 0.7 mm.min<sup>-1</sup>, and such values comply well with those obtained in previous studies performed  
 267 with spruce wood through cone calorimeter tests<sup>16</sup> and standard fire resistance tests.<sup>25,26</sup>  
 268 The in-depth char front propagation was measured for the entire width of the short panel as well as the  
 269 large panel by cutting the panels at every 5 cm height after each test and making direct measurements  
 270 of the char depth. **The steps for cutting the panel are presented in Fig. 12 and the results are shown in**  
 271 **Fig. 13 and 14 in the form of contour plots for tests with burner powers of 10, 20, 30, and 50 kW and**  
 272 **exposure times of 15 and 30 minutes.**



22 Figure 12: Steps for cutting the burning wood panel and measuring the location of the char front.

23  
24  
25 273 Figure 13 presents a comparison of the spatial profiles over the width of the char front depths on the  
26  
27 274 short and large panels at the height of 60 cm for a test performed at 30 kW after 30 minutes of exposure.  
28  
29  
30



51 Figure 13: Comparison of the spatial profile over the width of the char front depths in the small and large panels after 30  
52 minutes exposure to a 30 kW burner power.  
53  
54  
55

56 275 The char front depth profiles shown in Fig. 13 confirm the observations made by Zeinali *et al.*<sup>5</sup>  
57  
58  
59  
60

1  
2  
3 276 regarding the different thermal exposure on the small and large panel. Indeed, the average char front  
4  
5 277 depths in the small panel are always slightly higher than those in the large panel, indicating that the short  
6  
7 278 panel receives a slightly stronger thermal exposure, and this holds true for the entire panel width. **The**  
8  
9 279 **char front contours in Fig. 14 are based on experimental measurement (see protocol in Fig. 12). Thus,**  
10  
11 280 **each grid point corresponds to a direct measurement (at least 90 points per wood panel) and the contours**  
12  
13 281 **are plotted by interpolation between these data points.** In addition, Fig. 14 suggests that the area of  
14  
15 282 charring on the wood panels is larger than the area of high heat fluxes observed on incombustible panels,  
16  
17 283 especially at higher heights near the corner. This is due to the additional heat flux provided by the burning  
18  
19 284 of the wood panels and the higher flame heights in these tests compared to the tests with incombustible  
20  
21 285 panels.<sup>5,7</sup>

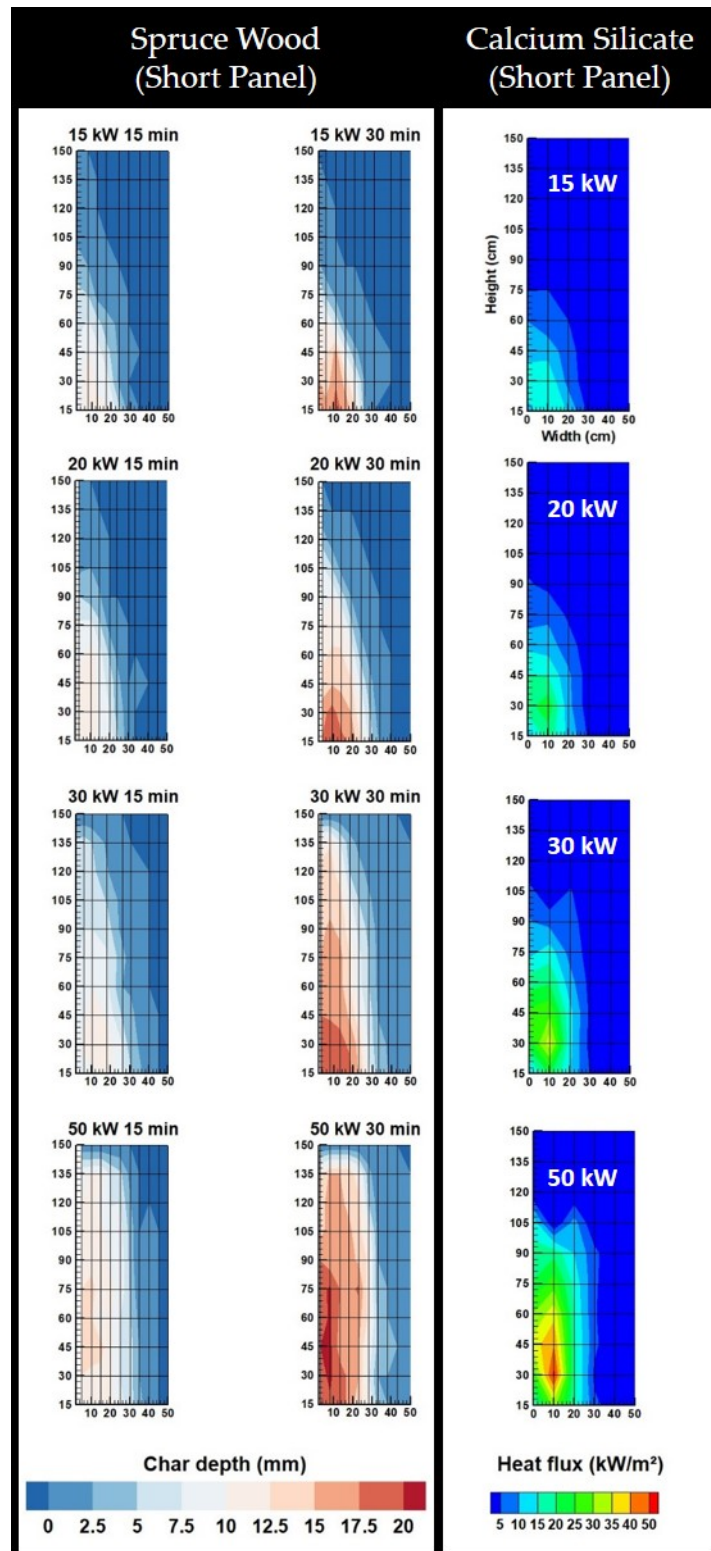
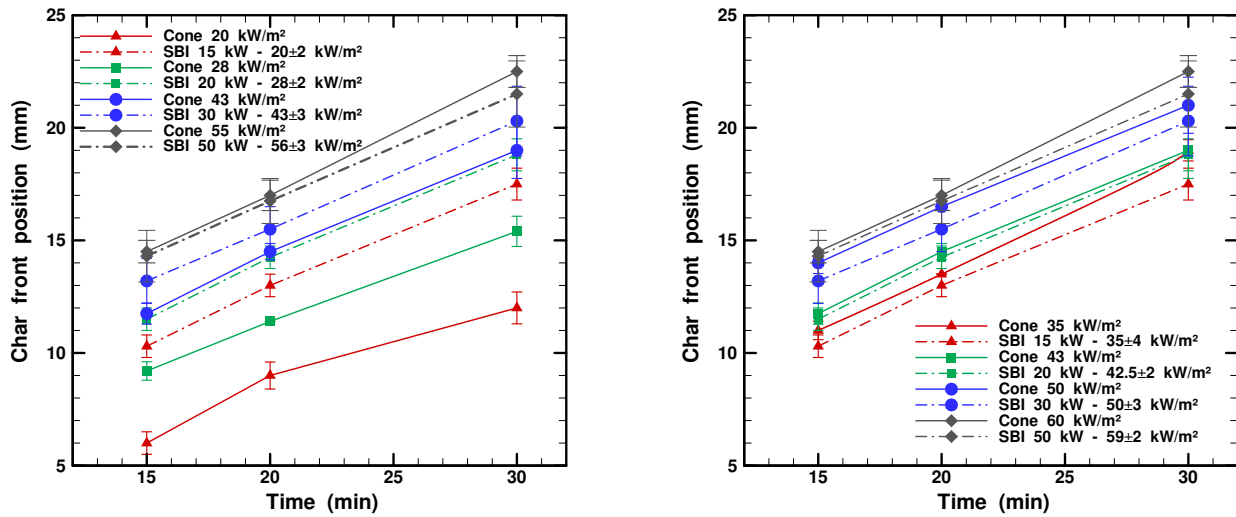


Figure 14: Contour plots of char front depths on a spruce wood panel (left) and contour plots of total heat fluxes on an incombustible panel (right) for burner powers of 15, 20, 30 and 50 kW.

### 286 *Comparison of in-depth charring in SBI and cone calorimeter tests*

287 Some additional experiments with the cone calorimeter<sup>4</sup> were performed in order to compare the  
288 wood degradation in this setup with that observed in the SBI setup. For the SBI, the burner's heat fluxes  
289 have a highly non-uniform pattern over the panels (see Fig. 3), whereas the heat fluxes of the cone heater  
290 have a quite uniform pattern over the sample in cone calorimeter tests.<sup>4</sup> Moreover, according to Fig. 4,  
291 adding a combustible panel can greatly increase the local heat flux (for a 15 kW burner power, the local  
292 heat flux was equal to 20 kW.m<sup>-2</sup> with the inert panel vs. 35 kW.m<sup>-2</sup> with the wood panel). This makes  
293 it difficult to compare the results of cone calorimeter and SBI tests. Having that in mind, the in-depth  
294 char positions of the two scales as a function of the heat flux and the exposure time were compared.  
295 For that, the spruce wood samples were exposed to seven constant heat fluxes at the cone calorimeter  
296 without igniter, namely 20, 28, 35, 43, 50, 55 and 60 kW.m<sup>-2</sup> for exposure times ranging from 15 to 30  
297 min. It should be noted that the auto-ignition did not occur for each heat flux but in any case smoldering  
298 combustion (char oxidation and glowing) occurred. After each test, the samples were cut in their middle  
299 and the position of the char depth was measured with a ruler. Figure 15 shows a comparison of the char  
300 front positions obtained with the SBI at position 9 shown in Fig. 3 and the char front positions obtained  
301 with the cone calorimeter using either the heat flux measured with an inert panel (Fig. 15a) or the heat  
302 flux measured with a wood panel (Fig. 15b).



(a) Comparison based on heat fluxes measured with the inert panels.

(b) Comparison based on heat fluxes measured with the wood panels.

Figure 15: Comparison of the char front position between the cone and the SBI as a function of time, for different heat fluxes measured at position 9 shown in Fig. 3. The error bars indicate the magnitude of deviation across three repeatability tests, and the symbols indicate the average values.

In Fig. 15a, where the reference of heat flux is based on inert panels, the char depth positions in SBI and cone tests are in good agreement for the highest heat flux (showing differences less than 2 mm), although the two tests involve very different scales. Nevertheless, for the lowest heat fluxes (20 and 28 kW.m<sup>-2</sup>), the char front positions are no more comparable since for these burner powers the heat flux measured on a wood panel differs significantly from the heat flux measured on an inert panel, as shown in Fig. 4. This explains the extended char depth in the SBI tests. In Fig. 15b where the reference of heat flux is based on wood panels, the comparison of the char front positions obtained at the SBI scale and at the cone scale shows better agreement between the two scales. The deviations for each heat flux are less than 2 mm between the SBI and the cone tests. These comparisons show that it would be more accurate to consider the heat flux with the wood panel for studying the scaling effect. However, results also show that for heat fluxes measured on the inert panel greater than 43 kW.m<sup>-2</sup>, it is possible to consider that the positions of the char front will be similar between the two scales. At lower heat fluxes, the modification of heat flux due to the burning of the wood panel is too large to predict the panel degradation from only the heat flux map measured on an inert panel.

## 317 CONCLUSIONS

318 The SBI was used to study the fire behavior of spruce wood at various burner powers and exposure  
319 times, i.e. beyond those defined in the standard of SBI.<sup>2</sup> Correspondingly, a total of 22 tests were per-  
320 formed with measurements including char depth, heat flux, in-depth temperatures with very thin thermo-  
321 couples (0.1 mm diameter) embedded inside wood panels as well as position of the char on the exposed  
322 surface. The heat fluxes measured with inert panels provided data about the distribution of total inci-  
323 dent heat fluxes over the panels for different burner powers. Accordingly, it was quantified how the heat  
324 flux distribution over the surface of the panels is non-uniform, with heat fluxes ranging from 1.5 to 50  
325 kW.m<sup>-2</sup>. The measured heat fluxes with wood panel were up to 85 % higher than the heat fluxes with  
326 an incombustible panel. For the highest burner powers, the total heat flux measured over the combustible  
327 panels was predominantly due to the burner power, rather than the burning of the panels themselves. This  
328 causes the heat fluxes to converge to those observed with incombustible panels. Indeed for these burner  
329 powers, the flame has already reached its maximum thickness and thus the heat flux cannot increase  
330 further. Moreover, high burner powers induce strong opposite flow of pyrolyzate mass over the surface,  
331 causing a so-called 'blowing effect' that leads to convective cooling.<sup>22</sup>

332 As demonstrated in some recent studies, the in-depth temperature can be underestimated when the ther-  
333 mocouple is not fixed in an appropriate way. Very thin thermocouples implanted along the isotherms  
334 were used in this study to quantify this underestimation and to accurately measure the in-depth temper-  
335 atures. As a result, it was found that the thermocouple wires implanted along the isotherms are faster to  
336 detect the rise of temperatures compared to the sheathed thermocouples placed in holes drilled from the  
337 back side, with up to 75 °C difference in the temperatures obtained using the two methods. Moreover,  
338 the position of the char front deduced from the 300 °C isotherm was found to comply very well with the  
339 direct measurements.

340 For the charring rate, a quasi-steady-state plateau between 0.6 and 0.7 mm.min<sup>-1</sup> was found while the  
341 propagation of the charring front on the exposed surface increased according to the exposure time and the  
342 burner power. In addition, it was found that the surface area of the highly degraded region varies linearly  
343 with the burner power for a fixed exposure time.

344 The comparison of the char front depth in the cone calorimeter and the SBI setup showed a good agree-  
345 ment for the higher heat fluxes. However, for the lower heat fluxes measured with an inert panel, there is  
346 a significant difference between the char front depths in SBI and cone tests, namely those of the SBI are



1  
2  
3 347 higher by nearly 100 % at an exposure time of 15 min, albeit the difference decreases to approximately 50  
4  
5 348 % for exposure times above 20 min. This difference is mainly due to the presence of flaming combustion  
6  
7 349 on the panels in the SBI tests. This suggests, for the study of the scaling change, to match the heat fluxes  
8  
9 350 for the cone calorimeter with those of the SBI test obtained with the wooden panel. However, the results  
10  
11 351 also show that when the heat fluxes are above  $43 \text{ kW}\cdot\text{m}^{-2}$ , the heat fluxes measured with incombustible  
12  
13 352 panels could be sufficient for the study of the change of scale.  
14

### 15 353 Declaration of conflicting interests

16  
17  
18 354 The author(s) declared no potential conflicts of interest with respect to the research, authorship, and/or  
19  
20 355 publication of this article.  
21  
22

### 23 356 References

- 24  
25  
26 357 [1] R. vanMierlo and B. Sette, “The single burning item (sbi) test method- a decade of development  
27  
28 358 and plans for the near future,” *Heron*, vol. 50, no. 4, pp. 191–208, 2005.  
29  
30 359 [2] E. Standard, “13823: 2013 reaction to fire tests for building products—building products excluding  
31  
32 360 floorings exposed to the thermal attack by a single burning item,” *AFNOR, ICS*, vol. 13, p. 50, 2002.  
33  
34 361 [3] ISO, “9705: International standard—fire tests—full-scale room test for surface products,” *International  
35  
36 362 Organization for Standardization, Geneva, Switzerland*, 1993.  
37  
38 363 [4] ISO, “5660-1: Reaction-to-fire tests – heat release, smoke production and mass loss rate – part 1:  
39  
40 364 Heat release rate (cone calorimeter method) and smoke production rate (dynamic measurement).,”  
41  
42 365 *International Organization for Standardization, Geneva, Switzerland*, 2015.  
43  
44 366 [5] D. Zeinali, S. Verstockt, T. Beji, G. Maragkos, J. Degroote, and B. Merci, “Experimental study of  
45  
46 367 corner fires part i: Inert panel tests,” *Combustion and Flame*, vol. 189, pp. 472–490, 2018.  
47  
48  
49 368 [6] J. Zhang, M. Delichatsios, and M. Colobert, “Assessment of fire dynamics simulator for heat flux  
50  
51 369 and flame heights predictions from fires in sbi tests,” *Fire Technology*, vol. 46, no. 2, pp. 291–306,  
52  
53 370 2010.  
54  
55  
56  
57  
58  
59  
60

- 1  
2  
3 371 [7] D. Zeinali, S. Verstockt, T. Beji, G. Maragkos, J. Degroote, and B. Merci, “Experimental study of  
4 372 corner fires part ii: Flame spread over mdf panels,” *Combustion and Flame*, vol. 189, pp. 491–505,  
5 373 2018.  
6  
7  
8  
9 374 [8] D. Lipinskas and R. Mačiulaitis, “Further opportunities for development of the method for fire origin  
10 375 prognosis,” *Journal of Civil Engineering and Management*, vol. 11, no. 4, pp. 299–307, 2005.  
11  
12  
13  
14 376 [9] P. Van Hees, T. Hertzberg, and A. Steen-Hansen, “Development of a screening method for the sbi  
15 377 and room corner using the cone calorimeter,” 2002.  
16  
17  
18 378 [10] A. S. Hansen and P. J. Hovde, “Prediction of time to flashover in the iso 9705 room corner test based  
19 379 on cone calorimeter test results,” *Fire and materials*, vol. 26, no. 2, pp. 77–86, 2002.  
20  
21  
22  
23 380 [11] M. A. Delichatsios, “Application of upward flame spread for the prediction of sbi and iso room  
24 381 corner (and parallel wall) experiments and classification,” *Thermal Science*, vol. 11, no. 2, pp. 7–  
25 382 22, 2007.  
26  
27  
28  
29 383 [12] T. Hakkarainen and M. A. Kokkala, “Application of a one-dimensional thermal flame spread model  
30 384 on predicting the rate of heat release in the sbi test,” *Fire and Materials*, vol. 25, no. 2, pp. 61–70,  
31 385 2001.  
32  
33  
34  
35 386 [13] J. Axelsson, P. Andersson, A. Lonnermark, P. Van Hees, and I. Wetterlund, “Uncertainties in mea-  
36 387 suring heat and smoke release rates in the room/corner test and the sbi,” *SP RAPPORTSTATENS*  
37 388 *PROVNINGSANSTALT*, vol. 2011:04, 2001.  
38  
39  
40  
41 389 [14] J. Axelsson and P. Van Hees, “New data for sandwich panels on the correlation between the sbi  
42 390 test method and the room corner reference scenario,” *Fire and Materials: An International Journal*,  
43 391 vol. 29, no. 1, pp. 53–59, 2005.  
44  
45  
46  
47  
48 392 [15] L. Tsantaridis, *Reaction to fire performance of wood and other building products*. PhD thesis,  
49 393 Byggvetenskap, 2003.  
50  
51  
52 394 [16] L. Terrei, Z. Acem, V. Marchetti, P. Lardet, P. Boulet, and G. Parent, “In-depth wood temperature  
53 395 measurement using embedded thin wire thermocouples in cone calorimeter tests,” *International*  
54 396 *Journal of Thermal Sciences*, p. 106686, 2020.  
55  
56  
57  
58  
59  
60

- 1  
2  
3  
4 397 [17] D. M. Chaudhari, G. J. Fiola, and S. I. Stoliarov, "Experimental analysis and modeling of buoyancy-  
5 398 driven flame spread on cast poly (methyl methacrylate) in corner configuration," *Polymer Degrada-  
6 399 tion and Stability*, vol. 183, p. 109433, 2021.  
8  
9  
10 400 [18] R. Fahrni, J. Schmid, M. Klippel, and A. Frangi, "Correct temperature measurements in fire exposed  
11 401 wood," in *World Conference on Timber Engineering (WCTE 2018)*, pp. MAT-O9, ETH Zurich,  
12 402 Institute of Structural Engineering (IBK), 2018.  
14  
15  
16 403 [19] R. Fahrni, J. Schmid, M. Klippel, and A. Frangi, "Investigation of different temperature measure-  
17 404 ment designs and installations in timber members as low conductive material," in *10th International  
18 405 Conference on Structures in Fire (SiF 2018)*, pp. 257–264, Belfast, United Kingdom, 2018.  
20  
21  
22 406 [20] P. Reszka and J. Torero, "In-depth temperature measurements in wood exposed to intense radiant  
23 407 energy," *Experimental Thermal and Fluid Science*, vol. 32, no. 7, pp. 1405–1411, 2008.  
25  
26  
27 408 [21] D. Drysdale, *An introduction to fire dynamics*. John Wiley & Sons, 2011.  
28  
29  
30 409 [22] J. G. Quintiere, "Fundamentals of fire phenomena," 2006.  
31  
32 410 [23] D. Zeinali, *Flame spread and fire behavior in a corner configuration*. PhD thesis, Ghent University,  
33 411 2019.  
35  
36 412 [24] H. C. Tran and R. H. White, "Burning rate of solid wood measured in a heat release rate calorimeter,"  
37 413 *Fire and materials*, vol. 16, no. 4, pp. 197–206, 1992.  
39  
40  
41 414 [25] A. Frangi and M. Fontana, "Charring rates and temperature profiles of wood sections," *Fire and  
42 415 Materials*, vol. 27, no. 2, pp. 91–102, 2003.  
44  
45 416 [26] I. ISO, "834: Fire resistance tests-elements of building construction," *International Organization  
46 417 for Standardization, Geneva, Switzerland*, 1999.  
48  
49  
50  
51  
52  
53  
54  
55  
56  
57  
58  
59  
60